Transmission of Helium Isotopes through Graphdiyne Pores: Tunneling Versus Zero Point Energy Effects

Marta I. Hernández,* Massimiliano Bartolomei, and José Campos-Martínez

Instituto de Física Fundamental, Consejo Superior de Investigaciones Científicas (IFF-CSIC), Serrano 123, 28006 Madrid, Spain

E-mail: marta@iff.csic.es

Abstract

Recent progress in the production of new two-dimensional (2D) nanoporous materials is attracting considerable interest for applications to isotope separation in gases. In this paper we report a computational study of the transmission of ^{4}He and ^{3}He through the (sub-nanometer) pores of graphdiyne, a recently synthesized 2D carbon material. The He-graphdiyne interaction is represented by a force field parametrized upon ab initio calculations and the ^{4}He/^{3}He selectivity is analyzed by tunneling-corrected transition state theory. We have found that both zero point energy (of the in-pore degrees of freedom) and tunneling effects play an extraordinary role at low temperatures ($\approx$ 20-30 K). However, both quantum features work in opposite directions in such a way that the selectivity ratio does not reach an acceptable value. Nevertheless, the efficiency of zero point energy is in general larger, so that ^{4}He tends to diffuse faster than ^{3}He through the graphdiyne membrane, with a maximum performance at 23 K. Moreover, it is found that the transmission rates are too small in the studied temperature

*To whom correspondence should be addressed

range, precluding practical applications. It is concluded that the role of the in-pore degrees of freedom should be included in computations of the transmission probabilities of molecules through nanoporous materials.

KEYWORDS: quantum sieving, nanoporous two-dimensional materials, Helium isotopes, graphdiyne, zero point energy, tunneling

Introduction

Recent advances in the fabrication of one-atom-thick membranes composed by nanometer or subnanometer size pores are allowing size-selective molecular separation applications.[1–3] As a noteworthy example, Koening *el al*[4] created sub-nanometer pores on a two-dimensional (2D) graphene membrane and were able to measure leak rates for various gases of small molecular weight, ranging from H_2 to SF_6. In these conditions (sub-nanometer pores, light molecules) one can expect that quantum effects such as tunneling and zero point energy (ZPE) may play a key role in the dynamics of the molecule passing through the pore. These features could be eventually exploited for isotopic separation, where the rate of permeation through the pore depends on the mass of the isotope (quantum sieving). In the case of helium, the lighter isotope, ^{3}He, is crucial for large neutron-scattering facilities as well as for experimental chemistry and physics,[5] so it is very important to progress in the development of new procedures for the separation of ^{3}He from the more abundant ^{4}He.

The role of zero point energy has been addressed in related studies of adsorption and diffusion of small molecules in microporous 3D materials.[6,7] A heavier isotope, with a smaller zero point energy, has a smaller "effective size" and therefore, it diffuses faster, as has been demonstrated, for instance, for the H_2/D_2 diffusion in a carbon molecular sieve by means of quasielastic neutron scattering studies.[8] Transition state theory (TST)[9] and molecular dynamic simulations with Feymann-Hibbs quantum corrections[6] are valuable aids for predicting the critical factors in the enhancement/inhibition of the transmission flux and thus, the mechanisms for a large selectivity ratio.

If the bottlenecks in the transmission/diffusion processes involve potential barriers, as is the case of subnanometer pores in 2D membranes, tunneling effects are also manifest. Recently, several studies have attempted to exploit this effect for the ^{3}He/^{4}He isotopic separation in the transmission of these species through various graphene derivatives[10–14] by means of one-dimensional calculations of the tunneling probabilities along the reaction path. Interestingly, tunneling goes on the opposite direction than the ZPE effect: transmission is

faster for the lighter species owing to a larger tunneling probability below the classical barrier. Therefore, for a given (temperature or pressure) condition the transmission process may become more efficient for one or the other isotope depending on which is the quantum effect dominating the dynamics. The interplay between ZPE and tunneling effects was recently studied by Schrier and collaborators,[15] who examined the feasibility for a thermally driven isotopic enrichment when ^{3}He and ^{4}He gases, at different temperatures, are separated by a nanoporous graphene membrane. As in the cited work, we believe that the degrees of freedom perpendicular to the reaction path must be included in the modeling of the transmission of light species through sub-nanometer 2D porous materials.

In this work we investigate the quantum effects in the transmission of ^{3}He and ^{4}He through a single graphdiyne sheet. Graphdiyne is a 2D carbon material formed by benzenic rings joined by chains composed of two acetylenic bonds (see Fig. 1), first proposed by Baughman *et al*[16] and recently synthesized.[17,18] It has been found that this new material has an acceptable mechanical resistance[19,20] and appealing electronic properties.[21] Interestingly, this membrane exhibits regularly distributed triangular pores of sub-nanometer size with promising properties for the filtration of molecules like H_2[21,22] or H_2O.[23] In a previous work,[14] some of us found, by means of accurate electronic structure calculations, that this material can be also adequate for the filtration of He from natural gas (chemical separation), and certainly superior than other graphene derivatives such as 2D polyphenylene honeycomb.[10,24] In that work we also investigated the ^{3}He/^{4}He isotopic separation by means of one-dimensional simulations of the tunneling probabilities and, as already mentioned, noted that the effect of the in-pore degrees of freedom should be added for a realistic simulation of the transmission process. Here we have developed a realistic model where those ZPE effects are taken into account within TST and, by adding tunneling corrections to the model, we have been able to assess the competition between ZPE and tunneling in the ^{3}He/^{4}He selectivity ratio as a function of the temperature.

At this point we would like to point out that throughout the discussions of this work

we will use the term "ZPE effects" in a lax manner to refer to the effects of the whole set of in-pore vibrational states, although the in-pore ground state is the most relevant one at sufficiently low temperatures.

The paper is organized as follows. Section 2 refers the computational methods used for the calculation of the transmission rate coefficients as well as gives an account of the model for the He-graphdiyne interaction potential. Results (rate coefficients and selectivity ratios) are reported in Section 3, discussion is given in Section 4 and finally a summary and an outlook is presented in Section 5.

Computational Methods

Transition State Theory

In this work it is considered that the bottleneck for the transmission of He atoms through a graphdiyne membrane is placed right at the center of a pore within the membrane plane. In addition, the reaction path is assumed to be a straight line crossing that point perpendicularly to the graphdiyne plane. Within Transition State Theory (TST),[9,25,26]the transmission rate can be written as a function of temperature T as

$$k(T) = \frac{k_B T}{h} \frac{Q^{\ddagger}}{Q_t} e^{-E_0/k_B T} f_{tunn}(T), \quad (1)$$

where k_B and h are the Boltzmann and the Planck constants, respectively, $Q^{\ddagger}$, the partition function at the transition state (TS), Q_t, the translational partition function of the He gas, and E_0 is the classical barrier height along the reaction path, which corresponds to the potential energy at the TS position. Specifically, the translational partition function is given by

$$Q_t = \left(\frac{m k_B T}{2\pi\hbar^2} \right)^{3/2}, \quad (2)$$

where m is the mass of the atom, and the TS partition function, by

$$Q^{\ddagger} = \sum_n e^{-E_n/k_BT}, \tag{3}$$

where E_n are the energy levels (with respect to E_0) of the bound states for the degrees of freedom perpendicular to the reaction path (He in-plane vibrations inside the pore).

Finally, $f_{tunn}(T)$ is a tunneling correction, given as the ratio between the classical (cl) and the quantal (q) rate coefficients along the one-dimensional (1D) reaction path:[25,26]

$$f_{tunn}(T) = \frac{k^q_{1D}(T)}{k^{cl}_{1D}(T)}, \tag{4}$$

where the 1D rate coefficients are given by

$$k_{1D}(T) = \left(\frac{1}{2\pi m k_B T}\right)^{1/2} \int e^{-E/k_BT} P(E) dE, \tag{5}$$

and $P(E)$ is the classical ($P^{cl}(E)$) or quantum ($P^q(E)$) transmission probability through the barrier of the reaction path, as a function of the kinetic energy E. The quantum transmission probability has been obtained from time-dependent wave packet calculations as described in detail in Ref.[14] Specifically, it is computed from the probability current at the barrier (z=0)[27,28]

$$P^q(E) = \frac{\hbar}{m} Im\left(\psi^{\star}_E(z=0)\frac{\partial \psi_E}{\partial z}|_{z=0}\right), \tag{6}$$

where ψ_E is the stationary wave function, which is obtained by means of a Fourier transform of the time-dependent wave packet. Computational details are as those reported elsewhere.[14] Finally, the classical probability is simply $P^{cl}(E) = \Theta(E - E_0)$, where $\Theta(x)$ is the Heaviside step function.

He-graphdiyne interaction potential

For a given position of He with respect to graphdiyne ($Gr2$), in Cartesian coordinates, the interaction potential is obtained as a sum over He-C pair potentials,

$$V_{He-Gr2}(x,y,z) \;=\; \sum_i V_{He-C}(R_i), \tag{7}$$

where R_i is the distance between He and the i^{th} carbon atom. The summation is performed over neighboring carbon atoms until convergence is reached (typically four significant digits on the total energy). The geometry of graphdiyne is that of Fig.1, with the following C-C bond lengths:[20] 1.431 Å and 1.231 Å for the aromatic and triple bonds, respectively, whereas 1.337 Å and 1.395 Å bond lengths were taken for the single bonds between two triple C-C bonds and for those atoms connecting aromatic and triple C-C bonds.

The pair potentials V_{He-C} were represented by the Improved Lennard-Jones (ILJ) formula:[29]

$$V_{He-C}(R_i) \;=\; \frac{\varepsilon}{n(\rho_i)-6}\left[6\rho_i^{-n(\rho_i)} - n(\rho_i)\rho_i^{-6}\right] \tag{8}$$

where $\rho_i = \frac{R_i}{R_m}$ is a reduced pair distance and $n(\rho_i) = \beta + 4.0\ \rho_i^2$. As such, this representation involves three parameters, R_m, ε and β, which take the values 3.595 Å, 1.209 meV and 7.5 (adimensional), respectively. These values where determined from an optimization procedure exploiting benchmark "coupled" supermolecular second-order Møller-Plesset (MP2C) perturbation theory[30] calculations, as described in detail elsewhere.[14]

The profile of the interaction potential along the reaction path (coordinate z) is shown in Fig. 2, whereas the dependence of this potential on the in-pore degrees of freedom is reported in Fig. 3, specifically, on the displacement from the pore center along the y coordinate, as shown in Fig. 1. In both cases the present potential is compared with ab initio MP2C calculations. It can be seen that the pairwise potential is in a quite satisfactory agreement

with the benchmark ab initio calculations. In particular, the potential barrier for the adopted potential is $E_0 = V_{He-Gr2}(0,0,0) = 36.92$ meV to be compared with 33.90 meV from the MP2C calculations. On the other hand, it is clear that, while the potential barrier is rather low at the center of the pore (reaction path), it rapidly becomes quite high as the atom separates from the pore center, indicating that the effective size of the pore might become rather small.

Results

In-pore bound states

Within the TST outlined in the previous Section, we first computed the exact (anharmonic) bound states of ^{4}He (m= 4.0026 amu) and ^{3}He (m= 3.016 amu) by diagonalization of the 2D Hamiltonian for the in-pore degrees of freedom x and y, at z=0:

$$H_{2D} = \frac{-\hbar^2}{2m}\left[\frac{\partial^2}{\partial x^2} + \frac{\partial^2}{\partial y^2}\right] + V_{He-Gr2}(x,y,0) \quad (9)$$

To this end, we used basis sets consisting of fixed-node discrete variable representation functions for the particle-in-a-box problem.[31] Resulting energy levels are reported in Table 1. It can be noticed that the zero point energy, 25.32 and 29.31 meV for ^{4}He- and ^{3}He, respectively, is quite large and of the same order of magnitude than the classical barrier height (36.92 meV). In addition, note that the ^{3}He ZPE is larger than that of the heavier isotope by a non-negligible amount. Therefore, it can be anticipated that, by means of the TS partition function (Eq. 3), the ZPE will play a relevant role in the transmission dynamics and that these effects will differ depending on the isotope under study.

Transmission rates coefficients

Transmission rate coefficients were computed using Eq. 1 in the temperature range from 20 to 100 K. Results are shown as black lines in Fig. 4 for ^{4}He (left panel) and ^{3}He (right panel). Although the rates increase very rapidly with temperature, they are extremely small for the lowest temperatures, indicating that actual transmission of He through graphdiyne would be very low in this range. Still, we are interested in this temperature range because quantum effects become more pronounced under these conditions. In this way, we study the effect of neglecting the in-pore degrees of freedom by assuming $Q^{\ddagger} = 1$ in Eq. 1 or, equivalently, setting the ZPE to zero. The results are shown as blue lines in Fig. 4, to be compared with the full calculation (black line). As can be seen, the in-pore degrees of freedom play a key role in lowering the values of the rate coefficients, especially at the lowest temperatures, a result already expected from the values of the frequencies at the Transition State (Table 1). As also expected, this effect is more pronounced for ^{3}He which has a larger ZPE. On the other hand, we analyze the role of tunneling by neglecting this effect in the computed rate coefficient (setting $f_{tunn} = 1$ in Eq. 1 but keeping $Q^{\ddagger}$ to its true value), and the resulting rates are depicted in Fig. 4 using red lines. By comparing with the full calculation, it can be seen that the role of tunneling is not remarkable except at the lowest temperatures. Again, note that the contribution due to tunneling is larger for the lighter isotope.

^{4}He/^{3}He selectivity

We turn now to compare the performance of the two isotopes. Looking at the black lines of the left and right panels of Fig. 4, it seems that the rate coefficients of both isomers are very close. In a way, it appears that ZPE and tunneling effects, being both larger for ^3He, compensate each other and the resulting rate coefficient is very close to that of the heavier isotope. To make a more detailed comparison, we consider the ^{4}He/^{3}He selectivity, $S_{4/3}(T)$, i.e., the ratio between the ^{4}He and ^{3}He rate coefficients (labels 4 and 3 refer to ^{4}He and ^{3}He, respectively)

$$S_{4/3}(T) = \frac{k_4(T)}{k_3(T)}. \tag{10}$$

In order to discriminate the effects due to ZPE to those due to tunneling and using Eq. 1, previous equation is rewritten as the ratio of a "4/3" selectivity due to the ZPE differences, $S^{zpe}_{4/3}$ (favoring ^{4}He so it is larger than one), and a "3/4" selectivity due to differences in the tunneling probabilities, $S^{tunn}_{3/4}$ (which is larger than one since ^{3}He tunneling is favored):

$$S_{4/3}(T) = \frac{S^{zpe}_{4/3}(T)}{S^{tunn}_{3/4}(T)}, \tag{11}$$

with

$$S^{zpe}_{4/3}(T) \;=\; \frac{Q^{\ddagger}_4(T)/Q_{t,4}(T)}{Q^{\ddagger}_3(T)/Q_{t,3}(T)}, \tag{12}$$

and

$$S^{tunn}_{3/4}(T) = \frac{1}{S^{tunn}_{4/3}(T)} = \frac{f_{tunn,3}(T)}{f_{tunn,4}(T)}. \tag{13}$$

Results are given in Fig. 5. It can be seen that the full selectivity $S_{4/3}$ (blue line) is always larger than one, indicating that the transmission of ^{4}He is faster than that of ^{3}He over the whole temperature range. This is due to the fact that the selectivity due to ZPE $S^{zpe}_{4/3}(T)$ (which favors the heavier species) is larger than $S^{tunn}_{3/4}(T)$, which would promote the lighter isotope due to the tunneling effect. It is worth noting that, although both contributions increase as temperature drops, the tunneling selectivity exhibits a much larger slope, suggesting that at $T << 20$ K, $S^{tunn}_{3/4} > S^{zpe}_{4/3}$, and the ^{3}He transmission would become more efficient. So far, we have not considered lower temperatures because of numerical innacuracies in the tunneling probabilities, since these probabilities become extremely small in the range of very small kinetic energies. Finally, note that, as a consequence of the behavior with temperature of these two quantum contributions, the ^{4}He/^{3}He selectivity reaches a maximum of 2.7 at 23 K.

Discussion

An important challenge for molecular separation applications is to achieve both a high selectivity and a high flux through the separating membrane. Roughly speaking, only molecules whose van der Waals (vdW) diameter is smaller than the pore size would be transmitted, leaving behind those molecules with larger vdW sizes. If the pore size is decreased, selectivity increases, but at the price of a much lower flux of the transmitting species. If the goal is to attain isotopic separation, the problem becomes even harder since one needs to rely on quantum effects, which are significant just at very low temperatures where transmission fluxes become very slow. In addition, we have shown that selectivities due to tunneling and ZPE quantum behavior go in opposite directions, so in the end, both effects compensate each other and the resulting selectivities are not high.

We have found that, for He-graphdiyne, ^{4}He diffuses faster than ^{3}He due to a larger importance of the ZPE quantum effects over tunneling over the 20-100 K temperature range. We believe that this is a correct prediction because the interaction potential used is realistic and the TST dynamical model employed has a sound physical ground. It is worth mentioning that the classical barrier for this system, $E_0 \approx 37$ meV, is of the same order of magnitude than some regarded as "low barriers" for other proposed 2D materials, such as partially nitrogen-functionalized porous graphene[11] (≈ 25 meV) and porous graphene-E-stilbene-1[32] (≈ 50 meV).

We would like to investigate whether a mild modification of the interaction potential (such that the barrier height varies between 25 to 50 meV) would increase the selectivity of one or another species (of He by an enhancement of the role of ZPE or rather of ^{3}He by an increase of the tunneling effects). To this end, we have set three model potentials labeled as $k = -1, 0, 1$, where the $k = 0$ case mimics the present He-graphdiyne interaction and $k = -1, 1$ are new scaled model potentials. The dependence with the z coordinate (reaction path) is defined as

$$V^{k}_{He-Gr2}(0,0,z) \;=\; f_k E_0 \;\exp\left[-\left(z/\Delta\right)^2\right]\left\{2\,\exp\left[-\ln 2\,\left(z/(f_k z_0)\right)^2\right]-1\right\}, \qquad (14)$$

where f_k is the scaling factor, varying as f_k= 0.75, 1, and 1.25 for $k = -1, 0, 1$, E_0= 36.92 meV (the He-graphdiyne barrier height), and Δ and z_0 have been set to 2.725 and 1.09 Å, respectively, to fit the actual profile of the He-graphdiyne potential. The resulting profiles are given in Fig. 6, where the present He-graphdiyne potential is also depicted (dashed lines) to show the quality of the analytical parametrization. As k increases, the barrier height goes from 27.7 to 46.2 meV, and the adsorption minima move from smaller to larger distances to the membrane plane, making the barriers wider. This is a trend previously found in several studies of the interaction between molecules and carbon-based nanoporous 2D materials.[23,33]

As a second ingredient of the model, we have assumed for simplicity that just the ground state is contributing to the TS partition function of Eq. 3. We have checked that this approximation holds up to the higher temperature range studied. Similarly to the reaction path potential, we have scaled the ZPE for the different cases using the same scaling factors f_k:

$$\mathrm{ZPE}(k) \;=\; f_k \cdot \mathrm{ZPE}_0 \qquad (15)$$

where ZPE_0 is the ZPE already reported in Table 1, i. e., 25.32 and 29.31 meV for ^{4}He and ^{3}He, respectively. In this way, we are assuming that, as f_k increases, we are simulating a pore that is becoming smaller in diameter and, accordingly, both the barrier height and the in-pore frequencies increase.

Further calculations of tunneling probabilities (Eq. 6), rate coefficients (Eq. 1) and selectivities (Eqs. 10-13) were performed within this model. In Fig. 7, we report the selectivities so obtained for the three interaction models $k = -1, 0, 1$. Several aspects may be discussed. First, the "4/3" selectivities due to ZPE effects (upper panel) are larger than

"3/4" selectivities due to tunneling (middle panel), so that the total selectivity (lower panel) is always favoring ^{4}He transmission in the studied temperature range. It is worth noting that the tunneling selectivities, $S_{3/4}^{tunn}$ exhibit a much smoother dependence with the scaling factor (f_k) and that the largest selectivity is reached for the interaction with the lowest barrier ($k = -1$). On the other hand, the largest ZPE selectivities $S_{4/3}^{zpe}$ are obtained for the highest barrier ($k = 1$) and, as a consequence, the largest total selectivity, $S_{4/3}$, is achieved for this potential, with a maximum of 4.8 at $\approx$ 20 K. Unfortunately, for this tight bottleneck the total flux would be impractically slow. Finally, note that, for the loose interaction ($k = -1$), $S_{4/3} \approx 1$ at 20 K and that it can be expected that, for $T < 20$ K, a non-negligible selectivity favoring ^{3}He transmission could be achieved. The results obtained for the $k = -1$ potential resemble very much those reported by Hauser *et al* for a two-ring-hole N_2-functionalized graphene pore,[12] although in the present case the selectivity is attenuated by the inclusion of the role of the ZPE.

Conclusion

In this work we have investigated the competition between zero point energy and tunneling effects in the transmission of ^{4}He and ^{3}He through a graphdiyne pore. A reliable force field, optimized from high level ab initio calculations, has been employed to describe the He-graphdiyne interaction, and transition state theory, including tunneling effects, has been used to compute transmission rate coefficients and selectivities. It is concluded that zero point energy and tunneling, being highly relevant quantum effects, somewhat compensate each other so that the transmission rate of one isotope does not significantly exceed that of the other isotope. In addition, it has been found that, in general, the influence of zero point energy overcomes that of tunneling, so that it is recommended that reaction path one-dimensional calculations should include the effect of the degrees of freedom perpendicular to the path, at least in an approximate manner.

The present study can be improved in several directions. First, transmission rate coefficients can be computed in a more accurate way by means of three-dimensional wave packet simulations. Further aspects could be studied within this approach, such as the effective size of the pores (with respect to the total area of the membrane) or the dependence of the dynamics on the angle of incidence of the He atoms. On the other hand, it would be interesting to analyze the performance of the vibrational degrees of freedom of the carbon atoms within the membrane. Work in these directions is in progress. Nevertheless, the design of a 2D membrane adequate for isotopic separation remains a tremendous challenge.

Acknowledgments

The work has been funded by Spanish MINECO grant FIS2013-48275-C2-1-P. Allocation of computing time by CESGA (Spain) and support by the COST-CMTS Action CM1405 "Molecules in Motion (MOLIM)" are also acknowledged.

References

(1) Huang, L.; Zhang, M.; Li, C.; Shi, G. Graphene-Based Membranes for Molecular Separation. *J. Phys. Chem. Lett.* **2015**, *6*, 2806–2815.

(2) Zhao, Y.; Xie, Y.; Liu, Z.; Wang, X.; Chai, Y.; Yan, F. Two-Dimensional Material Membranes: An Emerging Platform for Controllable Mass Transport Applications. *Small* **2014**, *10*, 4521–4542.

(3) Jiao, Y.; Du, A.; Hankel, M.; Smith, S. C. Modelling Carbon Membranes for Gas and Isotope Separation. *Phys. Chem. Chem. Phys.* **2013**, *15*, 4832–4843.

(4) Koenig, S. P.; Wang, L.; Pellegrino, J.; Bunch, J. S. Selective Molecular Sieving through Porous Graphene. *Nature Nanotechnology* **2012**, *7*, 728–732.

(5) Halperin, W. P. The Impact of Helium Shortages on Basic Research. *Nature Physics* **2014**, *10*, 467–470.

(6) Kumar, A. V. A.; Bathia, S. K. Quantum Effect Induced Reverse Kinetic Molecular Sieving in Microporous Materials. *Phys. Rev. Lett.* **2005**, *95*, 245901.

(7) Cai, J.; Xing, Y.; Zhao, X. Quantum Sieving: Feasibility and Challenges for the Separation of Hydrogen Isotopes in Nanoporous Materiasls. *RSC Advances* **2012**, *2*, 8579–8586.

(8) Nguyen, T. X.; Jobic, H.; Bathia, S. K. Microscopic Observation of Kinetic Molecular Sieving of Hydrogen Isotopes in a Nanoporous Material. *Phys. Rev. Lett.* **2010**, *105*, 085901.

(9) Hankel, M.; Zhang, H.; Nguyen, T. X.; Bhatia, S. K.; Gray, S. K.; Smith, S. C. Kinetic Modelling of Molecular Hydrogen Transport in Microporous Carbon Materials. *Phys. Chem. Chem. Phys.* **2011**, *13*, 7834–7844.

(10) Schrier, J. Helium Separation Using Porous Graphene Membranes. *J. Phys. Chem. Lett.* **2010**, *1*, 2284–2287.

(11) Hauser, A. W.; Schwerdtfeger, P. Nanoporous Graphene Membranes for Efficient ^{3}He/^{4}He Separation. *J. Phys. Chem. Lett.* **2012**, *3*, 209–213.

(12) Hauser, A. W.; Schrier, J.; Schwerdtfeger, P. Helium Tunneling through Nitrogen-Functionalized Graphene Pores: Pressure- and Temperature-Driven Approaches to Isotope Separation. *J. Phys. Chem. C* **2012**, *116*, 10819–10827.

(13) Mandrà, S.; Schrier, J.; Ceotto, M. Helium Isotope Enrichment by Resonant Tunneling through Nanoporous Graphene Bilayers. *J. Phys. Chem. A* **2014**, *118*, 6457–6465.

(14) Bartolomei, M.; Carmona-Novillo, E.; Hernández, M. I.; Campos-Martínez, J.; Pirani, F.; Giorgi, G. Graphdiyne Pores: "Ad Hoc" Openings for Helium Separation Applications. *J. Phys. Chem. C* **2014**, *118*, 29966–29972.

(15) Schrier, J.; McClain, J. Thremally-Driven Isotope Separation across Nanoporous Graphene. *Chem. Phys. Lett.* **2012**, *521*, 118–124.

(16) Baughman, R. H.; Eckhardt, H.; Kerte, M. Structure-Property Predictions for New Planar Forms of Carbon: Layered Phases Containing sp^2 and sp Atoms. *J. Chem. Phys.* **1987**, *87*, 6687–6699.

(17) Li, G.; Li, Y.; Liu, H.; Guo, Y.; Li, Y.; Zhu, D. Architecture of Graphdiyne Nanoscale Films. *Chem. Commun.* **2010**, *46*, 3256–3258.

(18) Zhou, J.; Gao, X.; Liu, R.; Xie, Z.; Yang, J.; Zhang, S.; Zhang, G.; Liu, H.; Li, Y.; Zhang, J.; Liu, Z. Synthesis of Graphdiyne Nanowalls Using Acetylenic Coupling Reaction. *J. Am. Chem. Soc.* **2015**, *137*, 7596–7599.

(19) Cranford, S. W.; Brommer, D. B.; Buehler, M. J. Extended Graphynes: Simple Scaling Laws for Stiffness, Strength and Fracture. *Nanoscale* **2012**, *4*, 7797–7809.

(20) Pei, Y. Mechanical Properties of Graphdiyne Sheet. *Physica B* **2012**, *407*, 4436–4439.

(21) Jiao, Y.; Du, A.; Hankel, M.; Zhu, Z.; Rudolph, V.; Smith, S. C. Graphdiyne: A Versatile Nanomaterial for Electronics and Hydrogen Purification. *Chem. Commun.* **2011**, *47*, 11843–11845.

(22) Cranford, S. W.; Buehler, M. J. Selective Hydrogen Purification through Graphdiyne under Ambient Temperature and Pressure. *Nanoscale* **2012**, *4*, 4587–4593.

(23) Bartolomei, M.; Carmona-Novillo, E.; Hernández, M. I.; Campos-Martínez, J.; Pirani, F.; Giorgi, G.; Yamashita, K. Penetration Barrier of Water through Graphynes'

Pores: First-Principles Predictions and Force Field Optimization. *J. Phys. Chem. Lett.* **2014**, *5*, 751–755.

(24) Blankenburg, S.; Bieri, M.; Fasel, R.; Müllen, K.; Pignedoli, C. A.; Passerone, D. Porous Graphene as Atmospheric Nanofilter. *Small* **2010**, *6*, 2266–2271.

(25) Truhlar, D. G.; Kuppermann, A. Exact and Approximate Quantum Mechanical Reaction Probabilities and Rate Constants for the Collinear H + H_2 Reaction. *J. Chem. Phys.* **1972**, *56*, 2232–2252.

(26) Garret, B. C.; Truhlar, D. G. Accuracy of Tunneling Corrections to Transition State Theory for Thermal Rate Constants of Atom Transfer Reactions. *J. Phys. Chem.* **1979**, *83*, 200–203.

(27) di Domenico, D.; Hernández, M. I.; Campos-Martínez, J. A Time-Dependent Wave Packet Approach for Reaction and Dissociation in H_2+H_2. *Chem. Phys. Lett.* **2001**, *342*, 177–184.

(28) Zhang, D.; Zhang, J. Z. H. Full-Dimensional Time-Dependent Treatment for Diatom-Diatom Reactions: The H_2+OH Reaction. *J. Chem. Phys.* **1991**, *101*, 1146–1156.

(29) Pirani, F.; Brizi, S.; Roncaratti, L.; Casavecchia, P.; Cappelletti, D.; Vecchiocattivi, F. Beyond the Lennard-Jones Model: A Simple and Accurate Potential Function Probed by High Resolution Scattering Data Useful for Molecular Dynamics Simulations. *Phys. Chem. Chem. Phys* **2008**, *10*, 5489–5503.

(30) Pitonák, M.; Hesselmann, A. Accurate Intermolecular Interaction Energies from a Combination of MP2 and TDDFT Response Theory. *J. Chem. Theory Comput.* **2010**, *6*, 168–178.

(31) Muckerman, J. T. Some Useful Discrete Variable Representations for Problems in Time-

Dependent and Time-Independent Quantum Mechanics. *Chem. Phys. Lett.* **1990**, *173*, 200–205.

(32) Brockway, A. M.; Schrier, J. Noble Gas Separation using PG-ESX (X=1,2,3) Nanoporous Two-Dimensional Polymers. *J. Phys. Chem. C* **2013**, *117*, 393–402.

(33) Bartolomei, M.; Carmona-Novillo, E.; Giorgi, G. First Principles Investigation of Hydrogen Physical Adsorption on Graphynes' Layers. *Carbon* **2015**, *95*, 1076–1081.

Table 1: Energy levels of the ^{4}He- and ^{3}He-graphdiyne bound states at the transition state. The zero of energy is defined at the maximum of the classical barrier along the reaction path, E_0, so that the energy of the ground state, $n = 1$, coincides with the zero point energy.

	Energy (meV)	
n	^{4}He	^{3}He
1	25.32	29.31
2	51.12	59.26
3	51.12	59.26
4	77.23	89.65
5	78.07	90.73
6	78.07	90.73
7	104.53	121.57
8	104.53	121.75
9	106.10	123.58
10	106.13	123.63

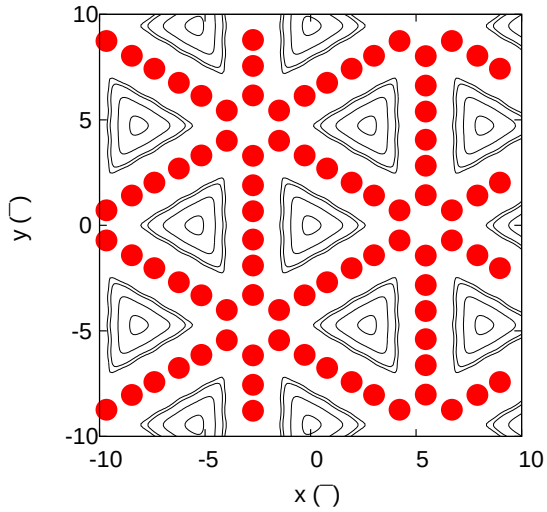

Figure 1: Scheme of the structure of graphdiyne. Carbon atoms are depicted by solid circles. Contour lines of the interaction potential at z= 0 are also displayed (contours are at 100, 1000, 5000 and 10000 meV).

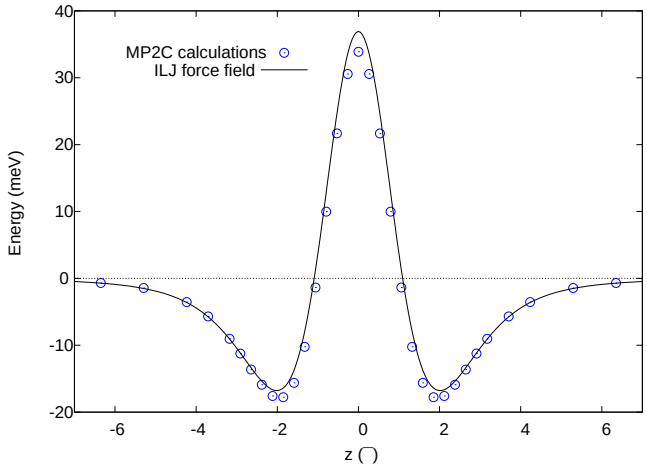

Figure 2: He-graphdiyne interaction potential $V_{He-Gr2}(0,0,z)$ (in meV) along the reaction path coordinate, z. The adopted Improved Lennard-Jones (ILJ) force field (lines) is compared with reference ab initio calculations using MP2C level of theory[14] (open circles).

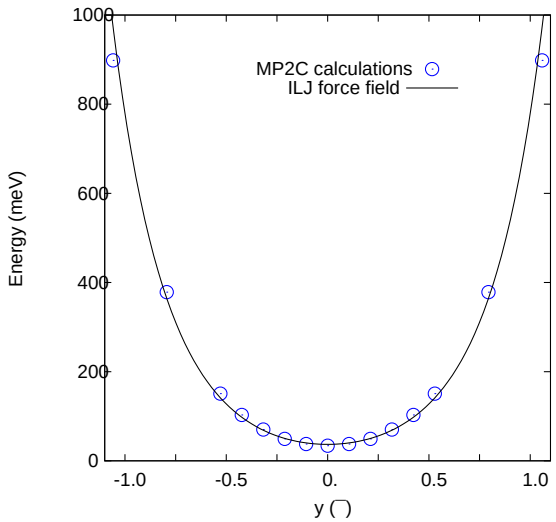

Figure 3: He-graphdiyne in-plane interaction potential, $V_{He-Gr2}(0, y, 0)$ (in meV), for the displacement of He from the pore center along the coordinate y (in Å). The adopted Improved Lennard-Jones (ILJ) force field (lines) is compared with reference ab initio calculations using MP2C level of theory[14] (open circles).

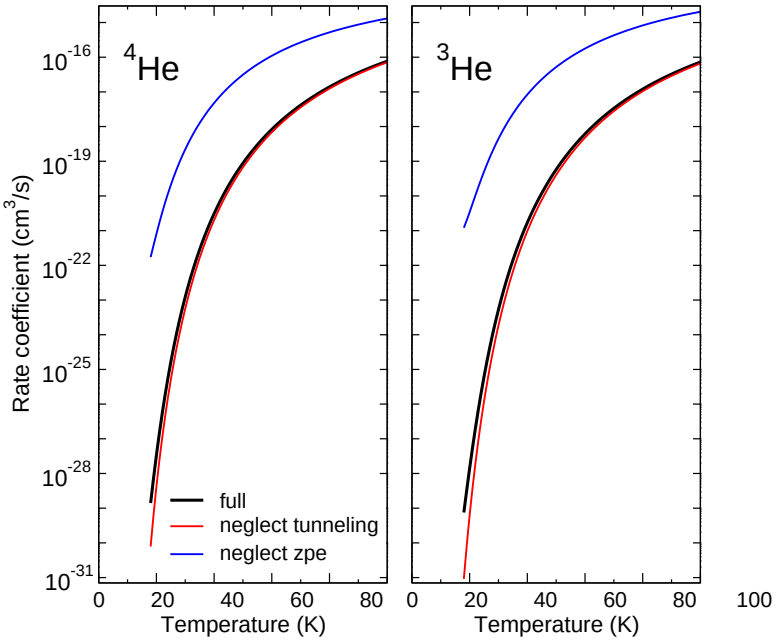

Figure 4: Rate coefficients (in cm^3s^{-1}) as functions of temperature for the transmission of ^{4}He (left panel) and ^{3}He (right panel) through a graphdiyne pore. Black lines give the TST result as in Eq.1, while blue lines correspond to the neglect of the ZPE at the transition state ($Q^{\ddagger}$=1) and red ones, to the neglect of tunneling effects (f_{tunn}=1).

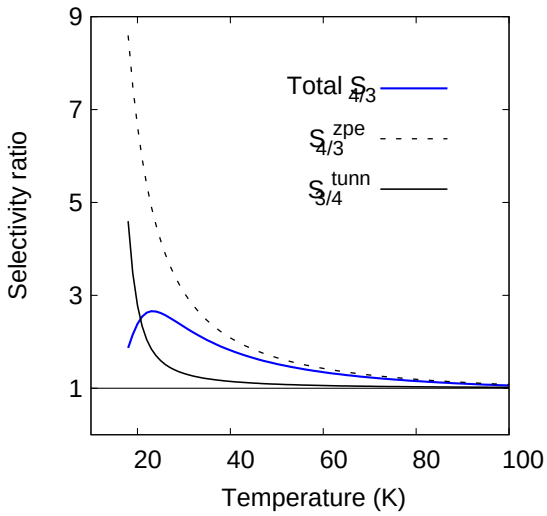

Figure 5: Selectivity ratio $S_{4/3}$ as a function of the temperature (blue line), as defined in Eq.10. The contribution due to the in-pore degrees of freedom, $S_{4/3}^{zpe}$, is shown using grey dashed lines whereas the tunneling contribution, $S_{3/4}^{tunn}$, is given by a black line.

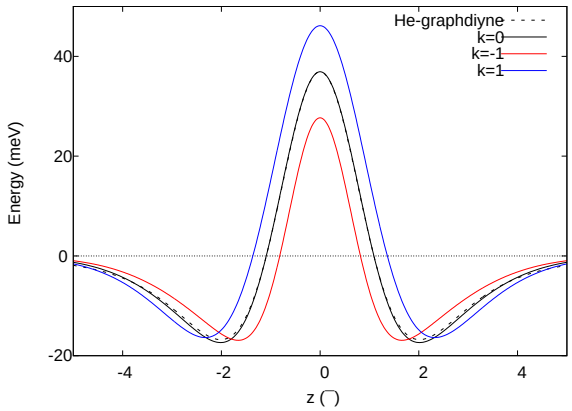

Figure 6: Interaction potentials V^k_{He-Gr2} for different scalings f_k= 0.75, 1., and 1.25 for k= -1, 0 and 1, respectively, (Eq. 14), as functions of the reaction path coordinate, z. The He-graphdiyne potential (Eq. 7) is also shown (dashed line) to be compared with the $k = 0$ case.

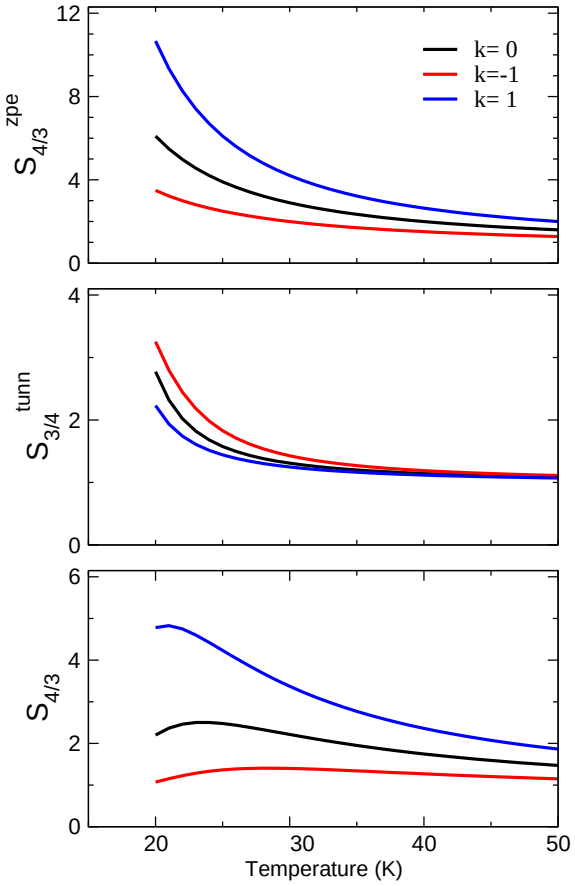

Figure 7: Selectivity ratios as functions of the temperature for the different interaction models with scalings f_k= 0.75, 1., and 1.25 for k= -1, 0 and 1, respectively (Eqs.14-15). Upper panel: Contribution due to the in-pore degrees of freedom, $S^{zpe}_{4/3}$. Middle panel: tunneling contribution, $S^{tunn}_{3/4}$. Lower panel: Total ^{4}He/^{3}He selectivity.